Inversion of Source Model of the 2011 off the Pacific Coast of Tohoku Earthquake Using Empirical Green's Function Method

T. Satoh
Shimizu Corporation, Japan

SUMMARY:
Source model composed of four strong motion generation areas (SMGAs) of the 2011 off the Pacific coast of Tohoku earthquake (*M*w9.0) is estimated using the empirical Green's function method. We also estimate the short period spectral level *A* of interplate earthquakes (*M*w6.0 to 7.8) including the aftershocks and foreshocks using the spectral inversion method. It is found that the *A* of the main shock calculated from the estimated source model is consistent with the empirical scaling estimated in our previous study and this study for interplate earthquakes with *M*w6.6 to 8.2. The SMGAs are located at deeper positions and are different from large slip areas. The total area of SMGAs S_a of the main shock is consistent with the empirical scaling by our previous study for interplate earthquakes with *M*w7.1 to 8.2. The empirical S_a is 1/5 of empirical total area of asperities derived by Murotani et al..

Keywords: The 2011 Tohoku earthquake, Source model, Empirical Green's function method, Scaling law

1. OBJECTIVES

The severe damage from tsunami and ground motions was caused during the 2011 off the Pacific coast of the Tohoku earthquake with *M*w9.0. In this study, toward the advancement of the strong motion prediction for interplate earthquakes, we estimate the source model composed of strong motion generation areas (SMGAs) using empirical Green's function method and calculate the short period spectral level from the source model. We also estimate the short-period spectral level of the foreshock, aftershock, and the other interplate earthquakes with *M*w6.0 to 7.8 on the Pacific plate in Japan using the spectral inversion method. The short-period spectral level is flat level of acceleration source spectrum (Dan et al., 2001) and is one of important parameters to strong motion prediction using fault models (e.g., Irikura and Miyake, 2011). Therefore we discuss the scaling law of the short-period spectral level with respect to seismic moment for the interplate earthquakes with *M*w6.0 to 9.0. In addition we examine whether the scaling law of the total area of SMGAs with respect to seismic moment derived from the interplate earthquakes with *M*w7.1 to 8.2 in our previous study (Satoh, 2010a) could apply to the main shock.

2. DATA AND METHOD

2.1. The Source Model of the Main Shock

Figure 2.1 shows the locations of epicenters by JMA and F-net CMT solutions by NIED of the main shock and two earthquakes used as empirical Green's functions together with 15 KiK-net strong motion stations by NIED used in the empirical Green's function method. To avoid the influence of nonlinearity of soil, borehole records at KiK-net stations are used. Locations of rupture starting points and ground motion generation areas (SMGAs) of the main shock estimated in this study are also shown in Fig. 2.1. We assume four SMGAs from analysis of the observed records. The 12/5/2005

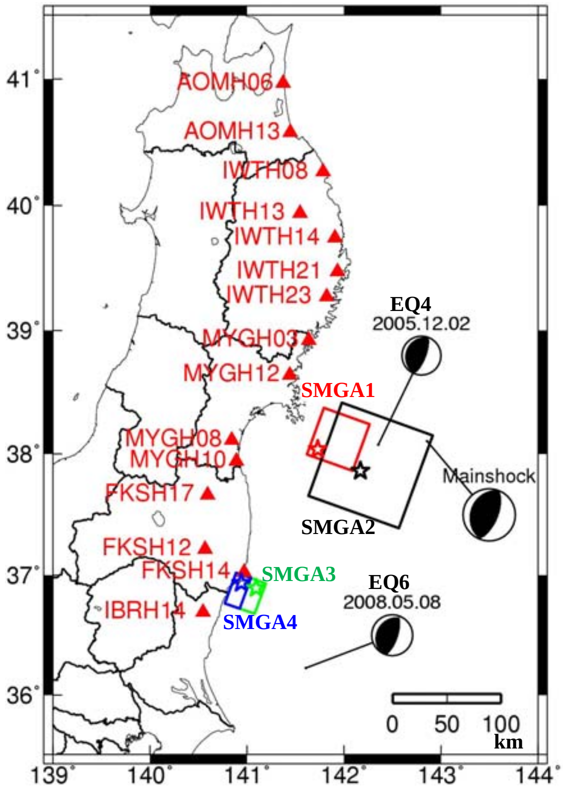

Figure 2.1. Epicenters and F-net CMT solutions of the main shock and the earthquakes used as the empirical Green's functions with location of KiK-net strong motion stations used for the source model estimation. Rectangles denote SMGAs and stars denote the rupture starting points estimated in this study.

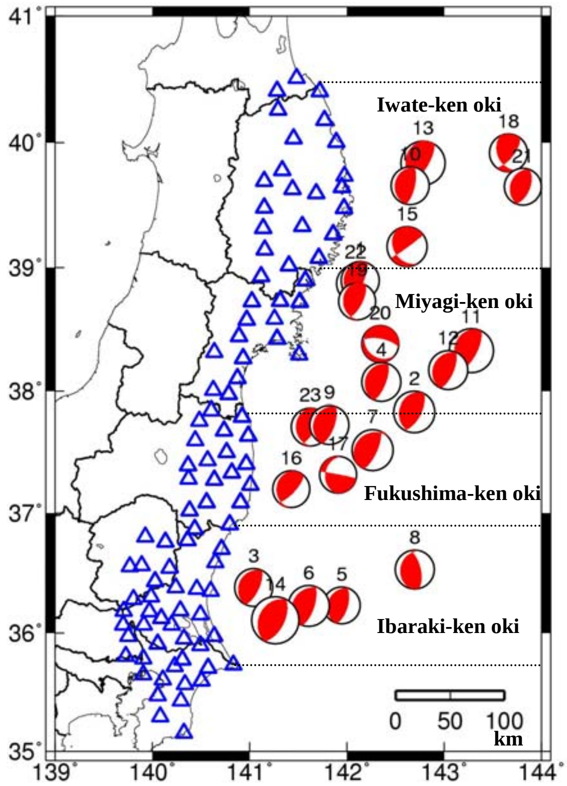

Figure 2.2. Epicenters and F-net CMT solutions of the interplate earthquakes together with location of K-NET strong motion stations used for the estimation of the short-period spectral level.

earthquake (EQ4) is used as the empirical Green's function for SMGA1 and SMGA2. The 5/8/2008 earthquake (EQ6) is used for SMGA3 and SMGA4. Element fault is defined as to be 15 x 15 km square based on the short-period spectral level of EQ4 and EQ6 shown in Table 2.1. The strike of the fault plane is assumed to be 200° based on F-net and the dip angle is assumed to be 15° as the subducting angle of the Pacific plate near the Japan arc.

We estimate the source model by the grid search method by Satoh (2010b) based on Miyake et al. (2003) using the empirical Green's function method by Dan and Sato (1998). We estimate the rupture starting point and the starting time for each SMGA by the method by Takenaka et al. (2006) and Suzuki and Iwata (2007) at the first step. Then we estimate the optimal values searching around them and parameters of four SMGAs using the grid search method. The optimal values are estimated to minimize the summation of normalized L2 norm between observed and synthetic seismograms. Here the envelope of 1 to 10 Hz acceleration records, 0.05 to 1 Hz velocity records, and 0.05 to 1 Hz displacement records are used to calculate the L2 norm.

2.2. The Short-period Spectral Level

Short-period spectral level A of the main shock is calculated from the estimated SMGAs using the equation (2.1) by Dan and Sato (1998).

$$A = 4\pi\beta^2 \left[\sum_{i=1}^{N} (\Delta\sigma_i r_i)^2 \right]^{1/2} \tag{2.1}$$

Here β is the S-wave velocity of the source (4.0 km/s), $\Delta\sigma_i$ is the stress drop of ith asperity, r_i is the equivalent radius of the ith asperity, N is the number of the asperities. We regard SMGAs as asperities.

Table 2.1. Source Parameters Used for the Estimation of Short Period Spectral Level *A*

Event	Origin Time*		Depth**	Source region*	M_0**	M_w**	A***
	Date	Hr:Mn	km		dyne・cm		dyne・cm/s^2
EQ1	2002.11.03	12:37	53	Miyagi-ken oki	3.87E+25	6.3	1.38E+26
EQ2	2003.10.31	10:06	26	Miyagi-ken oki	1.42E+26	6.7	9.88E+25
EQ3	2005.10.19	20:44	44	Ibaraki-ken oki	3.18E+25	6.3	1.21E+26
EQ4	2005.12.02	22:13	35	Miyagi-ken oki	5.39E+25	6.4	6.35E+25
EQ5	2008.05.08	1:02	26	Ibaraki-ken oki	2.12E+25	6.2	1.43E+26
EQ6	2008.05.08	1:45	35	Ibaraki-ken oki	1.97E+26	6.8	2.16E+26
EQ7	2008.07.19	11:39	35	Fukushima-ken oki	2.39E+26	6.9	1.31E+26
EQ8	2008.12.20	19:29	5	Ibaraki-ken oki	4.30E+25	6.4	5.78E+25
EQ9	2010.03.14	17:08	44	Fukushima-ken oki	6.83E+25	6.5	1.50E+26
EQ10	2010.07.05	6:55	38	Iwate-ken oki	2.79E+25	6.2	1.24E+26
EQ11	2011.03.09	11:45	23	Miyagi-ken oki	7.97E+26	7.2	5.97E+26
EQ12	2011.03.10	6:23	20	Miyagi-ken oki	5.51E+25	6.4	1.34E+26
EQ13	2011.03.11	15:08	35	Iwate-ken oki	1.40E+27	7.4	3.35E+26
EQ14	2011.03.11	15:15	35	Ibaraki-ken oki	5.66E+27	7.8	6.19E+26
EQ15	2011.03.11	20:36	38	Iwate-ken oki	8.33E+25	6.5	3.31E+26
EQ16	2011.03.12	22:15	44	Fukushima-ken oki	1.91E+25	6.1	7.93E+25
EQ17	2011.03.22	18:19	44	Fukushima-ken oki	1.65E+25	6.1	1.49E+26
EQ18	2011.03.22	18:44	11	Iwate-ken oki	3.01E+25	6.3	5.25E+25
EQ19	2011.03.25	20:36	44	Miyagi-ken oki	2.10E+25	6.1	8.44E+25
EQ20	2011.03.28	7:23	20	Miyagi-ken oki	1.66E+25	6.1	1.93E+26
EQ21	2011.04.14	4:57	17	Iwate-ken oki	1.39E+25	6.0	1.41E+26
EQ22	2011.07.23	13:34	47	Miyagi-ken oki	3.07E+25	6.3	1.43E+26
EQ23	2011.07.25	3:51	50	Fukushima-ken oki	2.96E+25	6.2	1.32E+26

*JMA **F-net ***This study

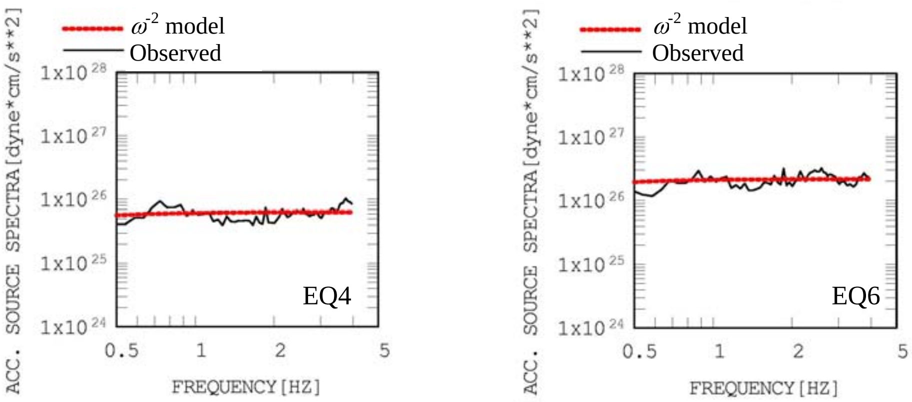

Figure 2.3. Comparison between observed acceleration source spectra and ω^{-2} model for EQ4 and EQ6 used as empirical Green's function method

Short-period spectral level of the other interplate earthquakes shown in Table 2.1. are estimated using empirical site amplification factors and *Q* values for path estimated using the spectral inversion method (e.g., Iwata and Irikura, 1988) by Satoh and Tatsumi (2002). The detailed method was shown in Satoh (2011). In Fig. 2.2. the locations of K-NET strong motion stations by NIED used to estimate the short-period spectral level are shown together with the epicenters by JMA and F-net CMT solutions by NIED. We select interplate earthquakes within the source region of the main shock with Mw≧6.0 and the focal depth of less than 60 km from earthquakes whose short-period spectral levels have not been estimated in previous studies.

Figure 2.3. shows the observed acceleration source spectra and ω^{-2} models of EQ4 and EQ6 used as the empirical Green's functions. The agreement between observed and model spectra is reasonably well. The flat level of the acceleration source spectra is the short period spectral level.

Table 3.1. Source Parameters of the Tohoku Earthquake

Parameter		SMGA1	SMGA2	SMGA3	SMGA4	Total SMGA
Length[km]		45.0	90.0	30.0	15.0	—
Width[km]		45.0	90.0	30.0	30.0	—
Area[km^2]		2025.0	8100.0	900.0	450.0	11475.0
Seismic Moment[dyne・cm]		1.49E+28	7.73E+28	3.23E+27	8.06E+26	9.63E+28
Stress Drop[bar]		397.7	258.5	291.0	205.7	—
Slip[cm]		1530.3	1989.5	746.6	373.2	—
Short-period Spectral Level[dyne・cm/s^2]		2.03E+27	2.64E+27	9.90E+26	4.95E+26	3.51E+27
Rupture Starting Time from Origin Time[s]		28.0	58.0	103.4	107.9	—
Rupture Velocity[km/s]		3.0	2.0	2.0	2.0	—
Rupture Starting Point	Longitude[°]	141.729	142.168	141.093	140.941	—
	Latitude[°]	38.036	37.863	36.892	36.937	—
	Depth「°]	48.0	36.6	50.9	54.8	—

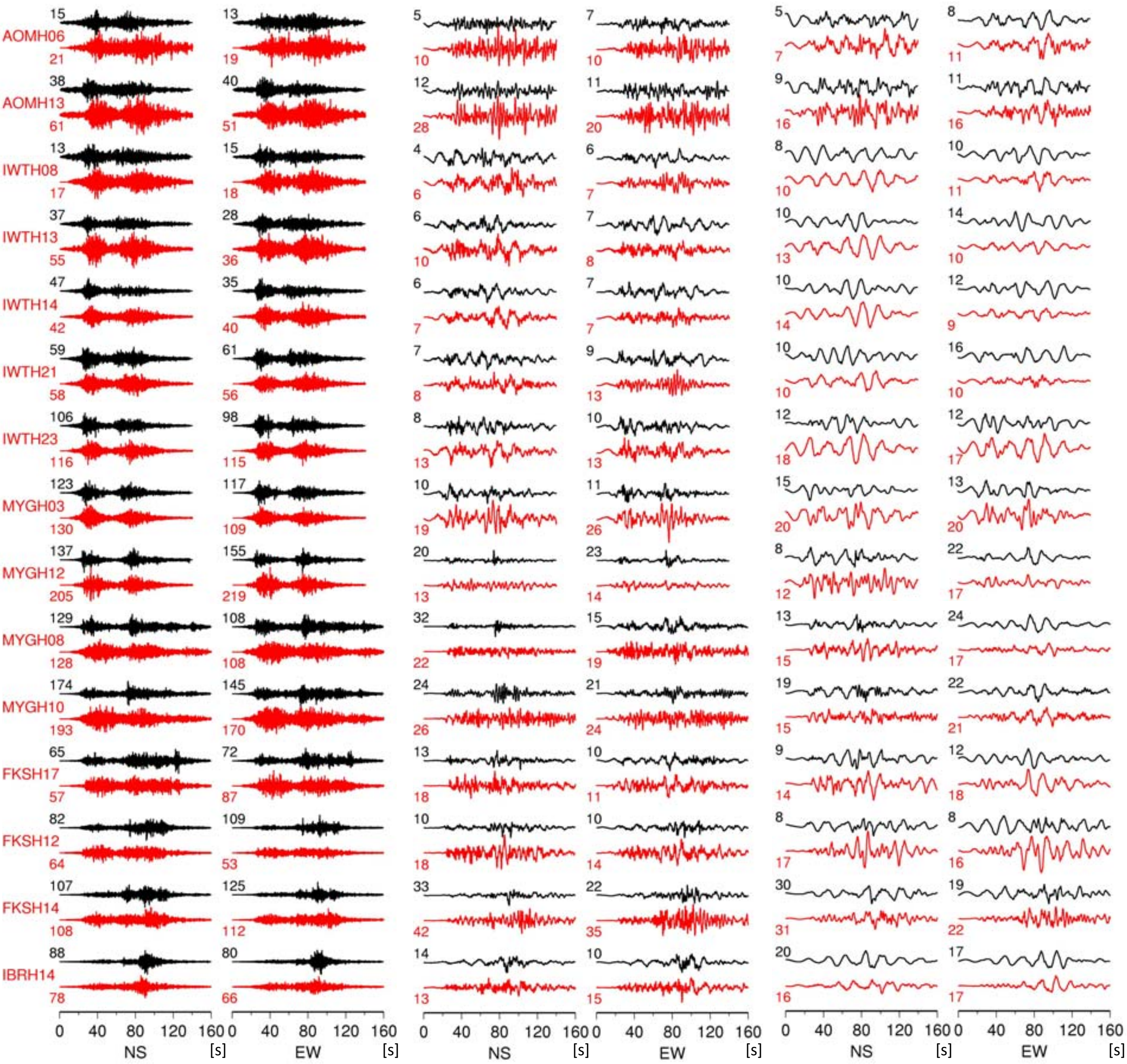

(a) 1 to 10 Hz Acceleration (b) 0.05～1Hz Velocity (c) 0.05 to1Hz Displacement

Figure 3.1. Comparison between observed (black lines) and the synthetic (red lines) seismograms.

3. RESULTS

3.1. The Source Model of the Main Shock

Table 3.1. shows the estimated source parameters of the main shock. The stress drop of the SMGA1 is largest among four SMGAs. All SMGAs are located west of the epicenter as shown in Figure 1. This location at deeper positions is different from large slip areas estimated from long-period strong motion records or teleseismic records (e.g., Yoshida et al., 2011a; Yoshida et al., 2011b). Large slip areas in these studies are mainly located east of the epicenter. Large slip areas estimated through tsunami data by Koketsu et al. (2011) are mainly located east of the epicenter similar to Yoshida et al.(2011a) and Yoshida et al.(2011b). However, large slip areas estimated through joint inversion of teleseismic, strong motion, and geodetic datasets by Koketsu et al. (2011) are overlapped to SMGA1 and SMGA2. These results suggest frequency-dependent rupture process as pointed out by several studies (e.g., Koper et al., 2011).

Figure 3.1. shows the observed and synthetic waves at KiK-net stations during the main shock. Number at the tip of each seismogram shows peak ground motion. The synthetic waves reasonably agree well with observed ones. Figure 3.2. shows synthetic acceleration wave calculated from each SMGA and the observed waves at FKSH17, FKSH14, and IBRH14. At IBRH14 synthetic waves from SMGA2, SMGA3, and SMGA4 are overlapped and so the duration with large acceleration are shorter than that at the other sites.

The SMGAs estimated by other researchers (Kamae and Kawabe, 2011; Asano and Iwata, 2011; Irikura and Kurahashi, 2012) using the empirical Green's function method are also located west of the epicenter. However, there is a SMGA located in Fukushima-ken oki in their source models, but not in our source model. In addition, area of SMGA2 in our model is larger than that of the SMGAs in Miyagi-ken oki in their models. In order to interpret the cause of the differences we divide SMGA2 into forward and backward side for FKSH17 and FKSH14 as shown in Fig. 3.3.(c) and calculate synthetic waves from both side. Figure 3.3. (a) and (b) show the acceleration seismograms generated from backward and forward side. It is found that the duration becomes longer by the backward waves at FKSH17 and FKSH14. The length of backward-side fault is long and the rupture velocity with 2.0 km/s is slow compared with those by the other researchers. Therefore the synthetic waves generated from the SMGA in Fukushima-ken oki in the other source models are interpreted to be mainly generated from backward side of large SMGA2 in our model.

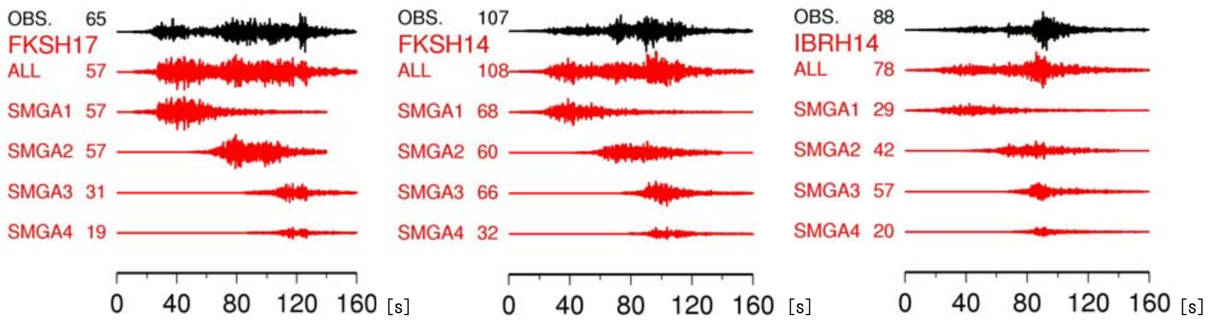

Figure 3.2. Comparison between observed (black lines) and the synthetic (red lines) acceleration waves (1 to 10 Hz) from all SMGAs and each SMGA.

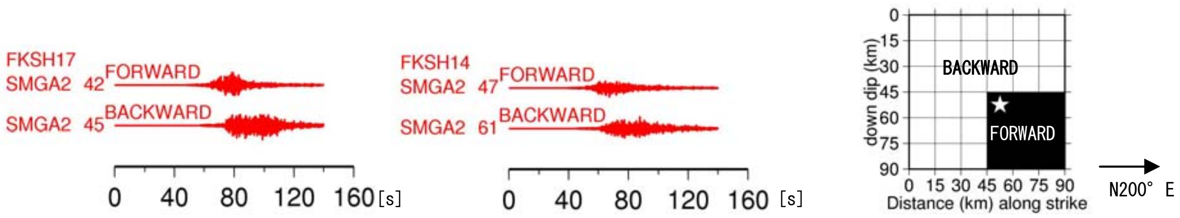

(a) Synthetic acceleration waves (b) Forward and backward potions

Figure 3.3. Comparison between the synthetic acceleration waves (1 to 10 Hz) from forward and backward potions of SMGA2 (a) and the location of the forward and backward potions of SMGA2 for two sites (b).

3.2. Scaling Law

Figure 3.4. shows the relations between the seismic moment M_0 and the short period spectral level A for interplate earthquakes on the Pacific plate in Japan. The A inverted in this study is consistent with the Satoh's (2010a) empirical relation for interplate earthquakes on the Pacific plate in Japan. The Satoh's (2010a) M_0-A relation is

$$A=4.02\times10^{17}M_0^{\ 1/3}, \tag{3.1}$$

which is about 1.6 times of Dan et al.'s relation (2001) for crustal earthquakes. It is also found that the A of big earthquakes (Mw>7) is different among regions. Especially, the A of earthquakes in Miyagi-ken oki tend to be large. The A of the 1978 Miyagi-ken oki earthquake, the 2005 Miyagi-ken oki earthquake and the foreshock EQ11 have similar M_0-A scaling which is slightly larger than the average + standard deviation of Satoh's (2010a) relation. The M_0-A relation of the main shock is consistent with extrapolation of average of Satoh's (2010a) relation. Here M_0 of the main shock is 4.0 $\times10^{29}$[dyne・cm] by Yoshida et al. (2011a) and Yoshida et al. (2011b).

Figure 3.5. shows the relations between M_0 and total area of SMGAs S_a for interplate earthquakes on the Pacific plate in Japan. The M_0-S_a relation for the main shock estimated in this study is consistent with extrapolation of Satoh's (2010a) empirical relation for interplate earthquakes on the Pacific plate in Japan. The Satoh's (2010a) M_0-S_a relation is

$$S_a=1.27\times10^{-16}M_0^{\ 2/3}, \tag{3.2}$$

which is about 1/5 times of Murotani et al.'s (2008) M_0-S_{asp} relation for interplate earthquakes on the Pacific plate and the Philippine Sea plate in Japan. Here S_{asp} is the total area of asperities. The definition of asperities by Murotani et al. (2008) are the zones of slips that are 1.5 times larger than the average slip estimated by waveform inversion. In the waveform inversion, data with period of longer than 2 to 5 seconds are mainly used. SMGAs are estimated by empirical Green's function method

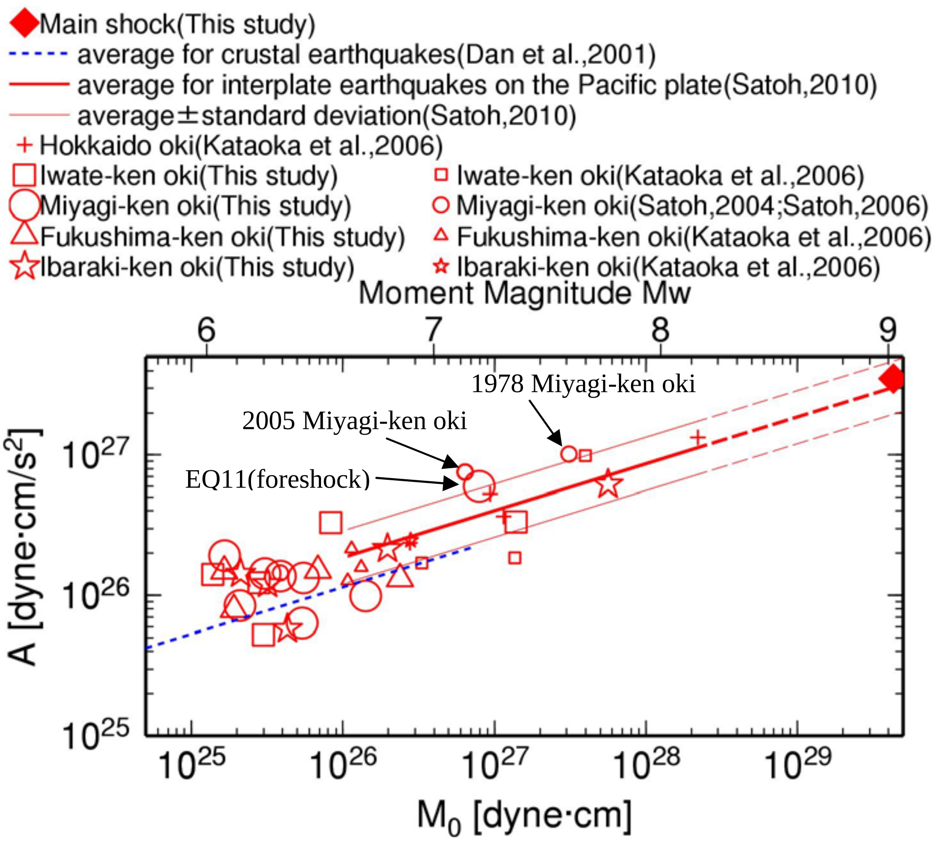

Figure 3.4. M_0-A relations for interplate earthquakes on the Pacific plate and those for crustal earthquakes

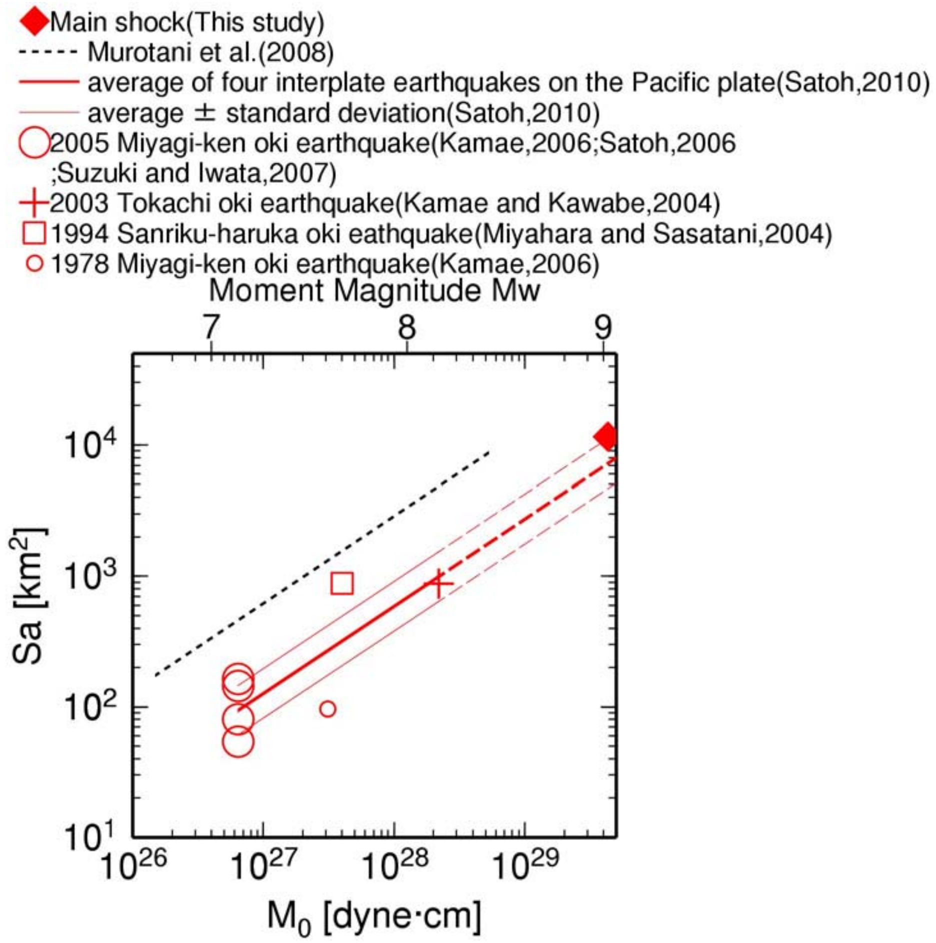

Figure 3.5. M_0-S_a relations for interplate earthquakes on the Pacific plate in this study and previous study. The black dashed line by Murotani et al.(2008) is M_0-S_{asp} relation for interplate earthquakes in Japan.

using broadband strong motion records in the period range from about 0.1 to 10 (or 20) seconds. Therefore the difference between S_{asp} and S_a is caused by the difference of main period range the difference of main period range of strong motions. These results also support frequency-dependent rupture process as pointed out by several studies (e.g., Koper et al., 2011).

4. CONCLUSIONS

Source model composed of four strong motion generation areas (SMGAs) of the 2011 off the Pacific coast of Tohoku earthquake (*M*w9.0) is estimated by the empirical Green's function method. We also estimate the short period spectral level *A* of interplate earthquakes (*M*w6.0 to 7.8) on the Pacific plate including the aftershocks and foreshocks by the spectral inversion method. The results are summarized as follows:

1) The short period spectral level of the main shock calculated from the estimated source model is consistent with the empirical scaling estimated in our previous study and this study for interplate earthquakes with *M*w6.6 to 8.2 on the Pacific plate in Japan.
2) The SMGAs of the main shock are located west of the epicenter. This feature is similar to SMGAs estimated using the empirical Green's function method by three groups (Kamae and Kawabe, 2011; Asano and Iwata, 2011; Irikura and Kurahashi, 2012) and are tend to be different from large slip areas estimated by waveform inversion using long-period waves or tsunami data.
3) The short period spectral level of big earthquakes (> *M*w7) occurred in Miyagi-ken oki tend to be large among the other interplate earthquakes on the Pacific plate in Japan.

4) The total area SMGAs S_a of the main shock is consistent with the empirical scaling in our previous study (Satoh, 2010a) for interplate earthquakes with *M*w7.1 to 8.2 on the Pacific plate in Japan. The total area SMGAs by Satoh (2010a) is 1/5 of the total area of asperities S_{asp} for interplate earthquakes in Japan by Murotani et al. (2008). The difference between S_{asp} and S_a is caused by the difference of main period range of strong motions generated from SMGAs and asperities.
5) The results of 2) and 4) support frequency-dependent rupture process as pointed out by previous several studies(e.g., Koper et al., 2011).

AKCNOWLEDGEMENT

This research was supported by JST on J-RAPID "Quantitative assessment of nonlinear soil response during the great Tohoku earthquake" (P.I. Prof. Kawase). Strong motion records observed at K-NET and KiK-net by NIED (National Research Institute for Earth Science and Disaster Prevention) are used. The CMT solutions by NIED and hypocenter information by Japan Meteorological Agency (JMA) are also used. I would like to thank these organizations to provide data and information. Some figures are plotted with GMT (Wessel and Smith, 1998).

REFERENCES

Asano, K. and Iwata, T. (2011). Strong ground motion generation during the 2011 off the Pacific coast of Tohoku Earthquake revealed by the broadmand strong motion simulation, http://sms.dpri.kyoto-u.ac.jp /k-asano/pdf/ssj2011_a11-06.pdf (in Japanese)

Dan, K. and Sato,T. (1998). Strong-Motion Prediction by. Semi-empirical method based on variable-slip rupture model of earthquake fault, *Journal of Structural and Construction Engineering* (*Transactions of the Architectural Institute of Japan*) **509**, 49–60.(in Japanese with English abstract)

Dan, K., Watanabe, M., Sato, T. and Ishii, T. (2001). Short-period source spectra inferred from variable-rupture models and modeling of earthquake faults for strong motion prediction, *Journal of Structural and Construction Engineering* (*Transactions of the Architectural Institute of Japan*) **545**, p51-62. (in Japanese with English abstract)

Irikura, K. and Miyake, H. (2011). Recipe for predicting strong ground motion from crustal earthquake scenarios, *Pure Appl. Geophys.* **168**, 85-104, doi:10.1007/s00024-010-0150-9.

Irikura, K. and Kurahashi, S. (2012). Strong ground motions during the 2011 Pacific coast off Tohoku, Japan Earthquake, http://www.kojiro-irikura.jp/pdf/One-year-after-the-2011-Tohoku_irikura_revised.pdf

Iwata, T. and Irikura, K. (1988). Source parameters of the 1983 Japan Sea earthquake sequence, *J. Phys. Earth* **36**, 155-184.

Kamae, K. and Kawabe, H. (2011). http://www.rri.kyoto-u.ac.jp/jishin/eq/tohoku3/SourceParaRev20110617.pdf (in Japanese)

Kataoka, S., Satoh, T., Matsumoto, S. and Kusakabe, T. (2006). Attenuation relations of ground motion intensity using short period level as a variable, *Journal of Structural and Earthquake Engineering, Japan Society of Civil Engineers* **62**:**4**, 740-757. (in Japanese with English abstract)

Koketsu, K., Yokota, Y., Nishimura, N., Yagi, T., Miyazaki, S., Satake, K., Fujii, Y., Miyake, H., Sakai, S., Yamanaka, Y. and Okada, T. (2011). A unified source model for the 2011 Tohoku earthquake, *Earth and Planetary Science Letters* **310**, 480-487, doi:10.1016/j.epsl.2011.09.009.

Koper, K.D., Hutko, A.R., Lay, T., Ammon, C.J. and Kanamori, H. (2011). Frequency-dependent rupture process of the 11 March 2011 M_W9.0 Tohoku earthquake: Comparison of short-period P wave backprojection images and broadband seismic rupture models, *Earth Planets Space* **63**, 599–602.

Miyahara, M. and Sasatani, T. (2004). Estimation of source process of the 1994 Sanriku Haruka-oki earthquake using empirical Green's function method, *Geophysical Bulletin of Hokkaido University* **67**, 197-212. (in Japanese with English abstract)

Miyake, H., Iwata, T. and Irikura, K. (2003). Source characterization for broadband ground-motion simulation: Kinematic heterogeneous source model and strong motion generation area, *Bull. Seismol. Soc. Am.* **93**, 2531-2545, doi:10.1785/0120020183.

Murotani, S., Miyake, H. and Koketsu, K. (2008). Scaling of characterized slip models for plate-boundary earthquakes, *Earth Planets Space* **60**, 987-991.

Satoh, T. (2004). Short-period spectral level of intraplate and interplate earthquakes occurring off Miyagi Prefecture, *Journal of Japan Association for Earthquake Engineering* **4:1**, 1-4. (in Japanese with English abstract)

Satoh, T. (2006). High-stress drop interplate and intraplate earthquakes occurred off shore of Miyagi prefecture, Japan, *Third International Symposium on the Effects of Surface Geology on Seismic Motion, Grenoble,*

France: 689-698.
Satoh, T. (2010a). Scaling law of short-period source spectra for crustal earthquakes in Japan considering style of faulting of dip-slip and strike-slip, *Journal of Structural and Construction Engineering* (*Transactions of the Architectural Institute of Japan*) **651**, 923-932. (in Japanese with English abstract)
Satoh, T. (2010b). Source modeing of the 2009 suruga bay earthquake using spectral inversion and empirical Green's function method, J*ournal of Structural and Construction Engineering* (*Transactions of the Architectural Institute of Japan*) **658**, 2153-2162. (in Japanese with English abstract)
Satoh, T. (2011). Scaling of short-period spectral level of accelerationsource spectra for aftershocks and foreshocks of the 2011 off the Pacific coast of Tohoku Earthquake, *Fourth IASPEI / IAEE International Symposium on the Effects of Surface Geology on Seismic Motion*, *Santa-Barbara, California*, 1.3_Satoh.pdf
Satoh, T. and Tatsumi, Y. (2002). Source, path, and site effects for crustal and subduction earthquakes inferred from strong motion records in Japan, *Journal of Structural and Construction Engineering* (T*ransactions of the Architectural Institute of Japan*) **556**, 15-24. (in Japanese with English abstract)
Suzuki, W. and Iwata, T. (2007). Source model of the 2005 Miyagi-Oki, Japan, earthquake estimated from broadband strong motions, *Earth Planets Space* **59**, 1155-1171.
Suzuki, W. and Iwata, T. (2009). Broadband seismic wave radiation process of the 2000 Western Tottori, Japan, earthquake revealed from wavelet domain inversion, *J. Geophys. Res*. **114**, B08302, doi:10.1029/2008 JB006130.
Takenaka, H., Nakamura, T., Yamamoto, Y., Toyokuni, G. and Kawase, H. (2006). Precise location of the fault plane and the onset of the main rupture of the 2005 west off Fukuoka prefecture earthquake, *Earth Planets Space* **58**, 75-80.
Wessel, P. and Smith, W.H.F. (1998). New, improved version of Generic Mapping Tools released, EOS, AGU.
Yoshida, Y., Ueno, H., Muto, D. and Aoki, S. (2011a). Source process of the 2011 off the Pacific coast of Tohoku earthquake with the combination of teleseismic and strong motion data, *Earth Planets Space* **63**, 571–576.
Yoshida, K., Miyakoshi, K. and Irikura, K. (2011b). Source process of the 2011 off the Pacific coast of Tohoku earthquake inferred from waveform inversion with long-period strong-motion records, *Earth Planets Space* **63**, 577–582.